Factors Affecting Y_2BaCuO_5 Precipitate Size During Melt Processing of $YBa_2Cu_3O_{7-x}$

C. VARANASI, P.J. MC GINN, and S. SENGUPTA

Center for Materials Science and Engineering, Department of Electrical Engineering, University of Notre Dame, Notre Dame, IN 46556

In the microstructures of melt processed $YBa_2Cu_3O_{7-x}$ (123) superconductors, often unconsumed Y_2BaCuO_5 (211) particles are observed. The 211 particle size and distribution depend upon i) processing parameters such as peak temperature, heating rate, residence time above 1010°C, starting 123 grain size, etc., ii) second phase additions, and iii) the processing route employed. 211 particle size control is of primary interest for enhancing 123 flux pinning, and fracture toughness. Factors which determine the 211 particle size are reviewed.

Keywords: Grain alignment (texturing), magnetization, Y_2BaCuO_5

INTRODUCTION

Melt processing of $YBa_2Cu_3O_{7-x}$ (123) is widely employed as a means to reduce the weak link behavior in order to obtain high critical current densities (J_c).[1-4] To further enhance the J_c of this high T_c superconducting oxide, it is necessary to provide flux pinning centers in the 123. Y_2BaCuO_5 (211) particles, which are always present in the melt textured microstructure due to incomplete peritectic reaction, have been noted to lead to improvements in the critical current density as long as they are below a critical size. This critical size has not been clearly identified, but it has been shown that large 211 precipitates tend to degrade 123 properties, while small 211 particles improve the properties.[5-9] A number of second phase additions[10-13] also have been found to provide additional flux pinning centers in 123. Often these second phase additions affect the morphology and the size of the 211 particles. Additions which refine and affect the 211 particle morphology, are of considerable interest as compared to the inert additions. The morphological changes of 211 particles as a result of the additions are important in light of the work of Wang et al.[14] where the presence of stacking faults has been related to the curvature of the 211 particles. Since stacking faults in 123 have been identified as potential flux pinning centers, the morphology of 211 particles that results in a maximum number of stacking faults will be preferred over others. There are many reports in the literature addressing other beneficial effects of 211 particles in the melt textured 123 microstructure. The 211 particles have been observed to assist in blunting the progress of cracks in the 123 matrix.[15] 211 particles were also reported[16] to enhance the fracture toughness of 123. It is clear from the above discussion that 211 particles play a significant role in melt textured 123 property enhancement and hence, the factors which affect the 211 particle size in melt textured 123 have been studied. Factors which have been found to influence the 211 size in melt textured 123 are shown in Table I. These factors are discussed in greater depth in the following sections.

(Received February 28, 1994)

PROCESSING ROUTES

Upon heating to above 1010°C, 123 decomposes peritectically into Y_2BaCuO_5 (known as the 211 phase), which is a nonsuperconducting phase, and a liquid phase consisting of Ba and Cu oxides. The 211 phase also peritectically decomposes when heated to above 1250°C into Y_2O_3 and another liquid consisting of Ba

Table I: Factors That Affect the 211 Particle Size

Processing Routes	Processing Parameters	Second Phase Additions	211 Particle Coarsening
[a]Melt Texture Growth	[a]Starting 123 grain size	[a]Additions which affect the 211 size by providing heterogeneous nucleation sites	[a]Ostwald ripening
[b]Liquid Phase Processing	[b]Heating rate	[b]Additions which affect the 211 size by chemical interactions	[b]Particle coalescence
[c]Quench Melt Growth	[c]Hold time		
[d]Zone Melt Texturing	[d]Superheating		
[e]Powder Melt Process			
[f]Solid Liquid Melt Growth			

and Cu oxides. Essentially all of the 123 melt processing routes involve a thermal excursion through the 123 peritectic temperature (1010°C) to produce a microstructure with reduced weak links. In all of the melt processes, Y_2BaCuO_5 phase remains in the final microstructure due to the incomplete peritectic reaction. The 211 particle size and volume, however, depend upon the processing techniques employed. The formation mechanism of 123 phase from the peritectic reaction considerably differs from the conventional peritectic reaction. Dissolution of a high temperature phase (211) in the liquid occurs to promote the formation of a low temperature phase (123), contrary to the conventional theory of the formation of low temperature phase in the form of a shell around the high temperature phase.[17,18] Accordingly, the smaller the 211 particle size is, the faster will be 123 formation, and thus the faster will be the processing speed.

Melt Texture Growth

This process[19] involves the use of stoichiometric 123 pellets, which are heated to temperatures above 1010°C. After holding for sufficient time to allow 123 decomposition to occur (10–20 min.), the pellets are initially slowly cooled at a rate of 1–12°C/h to 900°C in an applied temperature gradient of 20–50°C/cm and then quickly cooled to room temperature. The temperature gradient helps in aligning the grains by minimizing the random nucleation of 123 grains. 211 particles of 10–40 μm in size are typically found in the 123 microstructure.

Liquid Phase Processing

This process[20] involves the heating of stoichiometric 123 pellets to 1100°C, holding for a brief homogenization at 1100°C for 10 min, and then quickly cooling to 1030°C followed by a slow cool (1–2°C/h) to below the peritectic temperature. The quick cool to 1030°C helps in reducing the 211 particle coarsening time above the peritectic temperature. The pellets are then cooled at a relatively faster rate to room temperature. By following this melt processing route, one can minimize the number of 123 nucleation sites so that large domains of textured 123 can be obtained. No external temperature gradients are used in this process. 211 particles less than in 30 μm size can be produced in the 123 microstructure.

Quench Melt Growth/Melt Powder Melt Growth

This process[21] involves an initial quench of 123 material from 1400°C to room temperature and remelting the mixture at 1040°C followed by slow cooling to lower temperatures. The 211 phase dissociates above 1250°C into Y_2O_3 and a liquid phase consisting of oxides of Ba and Cu. Thus, the quenched material consists of Y_2O_3 particles in a glass matrix of Ba and Cu oxides. In a modified quench melt growth (QMG) process, the quenched material is crushed and mixed well before reheating for the sake of complete homogenization. This modified process[22] is known as the melt powder melt growth (MPMG) process. The quenched material is then heated to above 1010°C and slowly cooled through the peritectic similar to the earlier processes. During this process, the Pt contamination from the crucible combined with the quench process causes a considerable 211 particle size reduction. 211 particles with diameters less than 0.5 μm are observed in the 123 microstructure processed by this route.

Zone Melting

In this process,[23] sintered wires of 123 material are passed slowly (R = 2–3 mm/h) through a heat source maintained at temperatures above 1010°C. The temperature gradient depends upon the type of heating source used, and the design of cooling coils at the exit end of the heat source. Generally, laser heating provides high temperature gradients (G) in excess of 1000°C/mm as compared to 30°C/mm obtained in a resistively heated furnace. According to constitutional supercooling theory, gradient (G)/pulling rate(R), or (G/R ratio), determines the growth front morphology where a high G/R ratio favors a planar front growth. However, recent theories based upon 211 particle dissolution in liquid to control 123 growth, show that the magnitude of the thermal gradient has only a

minor effect on the maximum growth rate for planar solidification.[24] A modification of vertical zone melting is the horizontal Bridgman technique[25] where the wires are placed in a boat which is passed through a temperature profile in a furnace to get texture along the length of the wire.

211 particles of 10–40 μm in size are seen in 123 microstructures processed by zone melt processing using a resistively heated furnace. However, if laser heating is used instead of resistive heating, much finer 211 size can be expected due to the rapid heating rates involved (in the section on Heating Rate During Processing, the effects of heating rate are discussed). In zone melt processing, the rate of heating and cooling are approximately the same as 123 wire is made to pass through a fixed temperature gradient at a fixed rate. However, due to the presence of extra cooling coils at the exit end of the wire, cooling rates maybe higher than the heating rates. Calculation of the cooling rate gives a value of 90°C/h (G = 30°C/mm, R = 3 mm/h; cooling rate = G × R = 90°C/h), which is 90 times as fast as that used during melt texturing of a pellet (cooling rate 1°C/h). Since the cooling rates are relatively high in zone melting processing, the 211 particle dissolution time in the liquid during the formation of 123 are reduced. Due to this, a greater number of coarse 211 particles can be entrapped in zone melt processed 123 wires as compared to melt textured 123 pellets.

When pellets are rapidly heated by inserting them into a preheated furnace during melt texturing, heating rates of ~250°C/min are achieved. This heating rate is nearly 170 times that used in zone melt processing (~90°C/h). Since a faster heating rate produces fine 211 particles (see section on Heating Rate During Processing), the initial 211 particle size in the pellets before the actual texturing process is much finer as compared to that in the wires during zone melt texturing.

The residence time at 1040°C is approximately 3 h in zone melting, as compared to ~30 min in pellet melt texturing. The residence time at 1040°C in zone melt processing can be calculated by dividing the hot zone length (~1 cm) by the traveling speed (3 mm/h) in the case of a resistance furnace zone melter. Also, a step in the cooling cycle in pellet texturing is generally used which is absent in zone melt processing. All these factors contribute to differences in the extent of 211 particle coarsening in pellets and wires processed by melt texturing and zone melting respectively.

Powder Melt Process

Powder melt process (PMP)[26] refers to the melt processing of textured 123 starting with a mixture of 211 and a liquid composition. The mixture of externally prepared 211 and the liquid composition powders is heated to above 1040°C for a brief period and then cooled slowly through the peritectic temperature in a temperature gradient. Critical current densities of the order of 10^5 A/cm^2 have been obtained by using this process. In 123 processed by the PMP route, 211 particles with an average size of 0.4–0.8 μm are observed when solid state prepared 211 was used. However, one can still probably further reduce the final 211 particle size by starting with even finer sized 211 as a precursor.

Solid Liquid Melt Textured Growth

In this process,[27-29] one starts with calculated amounts of Y_2O_3, $BaCuO_2$, CuO to produce 123 or 123/211 composite materials. The powder mixture is heated rapidly at a rate of (250°C/min) to above 1030°C and kept for 10 min and slowly cooled through the peritectic at a rate of 1°C/h. Less than 100 nm size 211 particles as well as 1–10 μm sized 211 particles are found in 123 processed by this process. Using an atomic force microscope (AFM), the 100 nm sized 211 particles can be easily seen by scanning across a cleaved 123 domain as shown in Fig. 1.

MELT PROCESSING PARAMETERS

Starting 123 Grain Size

Varanasi et al.[30] observed that the 211 particle size depends on the initial 123 grain size. By increasing the sintering temperature, the 123 grain size increased, and correspondingly an increase in the 211 size was observed in melt textured 123. The microstructures of samples which were quenched from

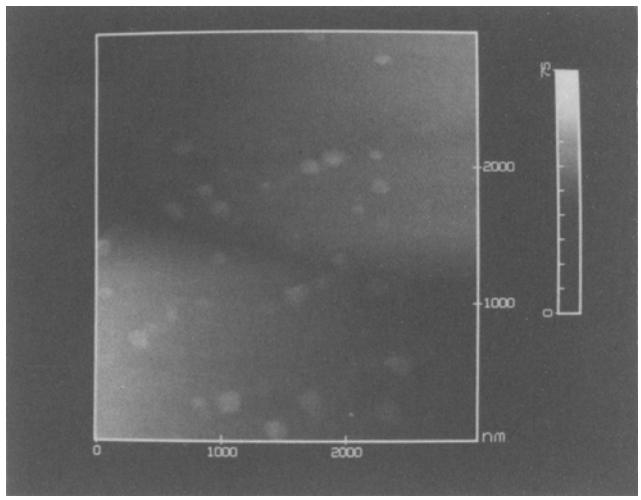

Fig. 1. Atomic force microscope image generated by scanning a cleaved domain of a SLMG sample showing the presence of fine (<100 nm) 211 particles.

Table II: Variation of 211 Particle Size as a Function of Starting 123 Grain Size*

123 Grain Size (μm)	Mean 211 Particle Length (μm)	Mean 211 Particle Width (μm)
2.6	30.0	6.9
8.0	47.6	10.4
55	93.4	16.2

*Griffith et al.

1040°C also indicated this dependence of 211 size on the initial 123 grain size. From these results, it was concluded that the nucleation and growth of 211, in the absence of any second phase additions which might act as heterogeneous nucleation sites (as discussed later), depends upon the 123 grain size. The mechanism by which the 211 forms with decomposition of 123 is still unclear, but these results point to, for example, decomposition initiating at sites such as grain triple point junctions or along the grain boundaries in the 123 microstructure. In such a case, as the 123 grain size decreases, there will be more potential nucleation sites, so that more 211 particles, and of a finer size, will be produced. Thus, all else being equal, finer 211 can be produced in a sample that starts with finer 123. Quantitative analyses by Griffith et al.[31] (see Table II) on 211 particles produced by decomposing 123 of various starting grain sizes, shows this effect clearly.

Table III: Variation of 211 Particle Size as a Function of Heating Rate*

Heating Rate (K/h)	Avg. Size of 211 (μm)	Volume Fraction of 211 (%)
60	20–25	20–23
3600	5–12	22–26
$>10^5$	2–4	26–29

*Rignalda et al.

Heating Rate During Processing

As the heating rate during 123 melt processing is increased, the final 211 particle size in the melt textured 123 is observed to decrease. The faster the Y-123 is heated above the peritectic (to 1050°C, for example) the higher the temperatures that can be achieved before 123 decomposition begins. Thus, the 123 becomes more unstable. The higher instability accelerates the precipitation and thus results in a larger density of nucleation sites, resulting in the production of finer 211.[32] Thus, in normal melt texture growth, a more rapid heating rate will yield finer 211 in the textured microstructure, assuming the subsequent cooling rate is kept constant for all the experiments. Rignalda et al.[32] have measured (see Table III) the 211 size variations as a function of the heating rate.

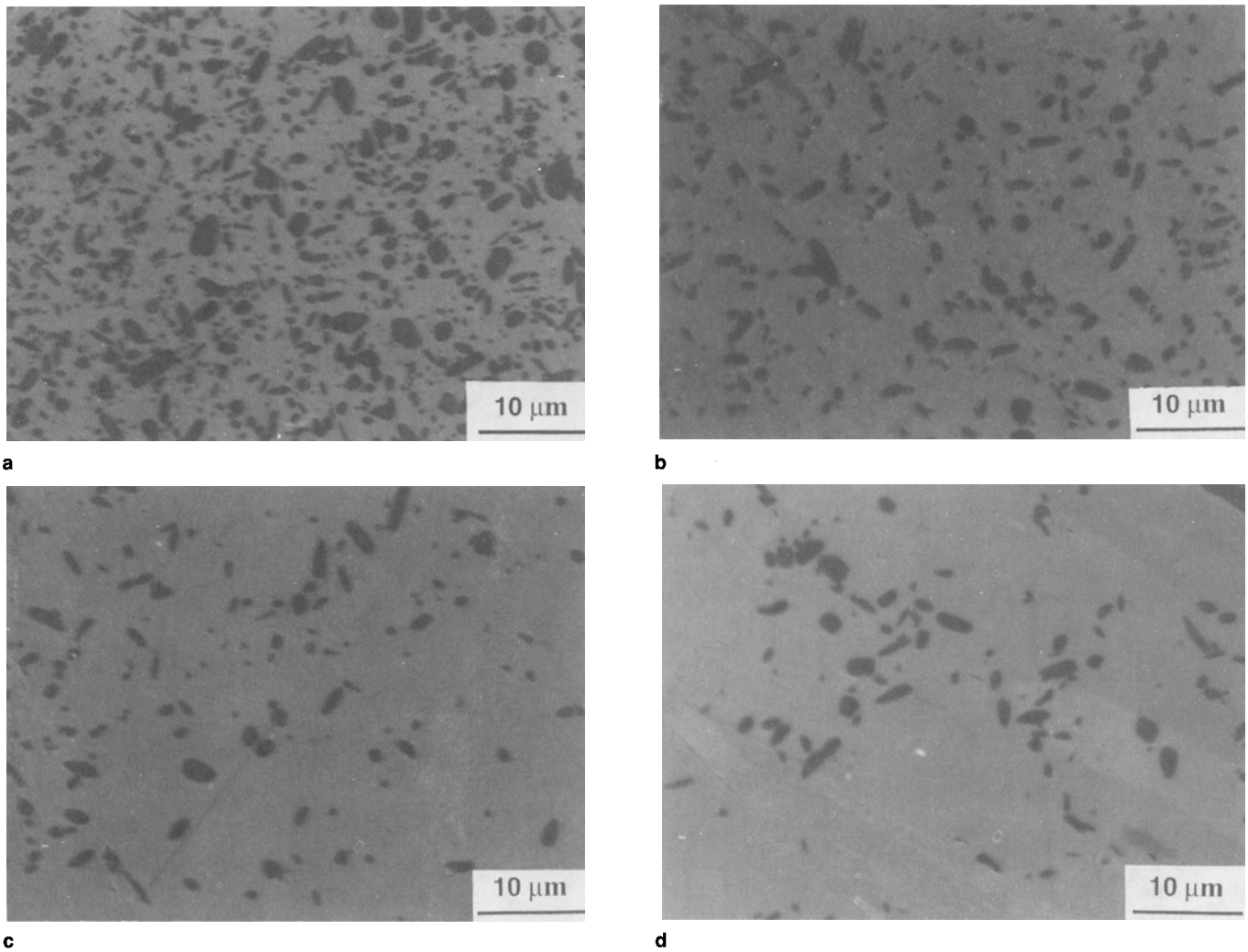

Fig. 2. Optical photomicrographs of melt textured pure 123 samples held at 1040°C prior to the cooling cycle for (a) 0.5, (b) 2, (c) 5, and (d) 10h.

Hold Time Above the Peritectic Temperature

Little work has been reported in the literature on the effect of hold time above the peritectic temperature on the resulting 211 size and 123 properties. To study this effect, the 123 hold time above Tp was varied from 30 min to 10 h during normal melt texturing cycle. In this study, a heating rate of 250°C/min was maintained for all the samples. Following the earlier discussion, using an identical starting 123 powder particle size (2–5 μm) to make the pellet samples is expected to give rise to a similar 211 particle size above the peritectic (Tp) when the heating rates are equivalent. If the heating rate is low, the effect caused by the hold time above Tp will not be prominent enough to be noticed as considerable coarsening will occur during the heat up. When the heating rates are high (250°C/min), one expects to produce fine 211 particles, and as the time of hold is increased, due to Ostwald ripening, these fine particles will be consumed as the big particles grow. This effect will not be readily observed if the starting 211 particle size is already large due to the slow heating rates of 123 samples. This is thought to be one of the reasons why Rignalda et al.[32] who used slow heating rates, did not notice the 211 particle size differences in melt textured 123 as the hold time was varied.

A microstructural examination of melt textured 123 pellets held at 1040°C for 30 min, 2 h, 5 h, and 10 h, during a normal melt texture cycle (i.e. 1°C/h cooling to 950 from 1005°C), revealed that the large 211 particles (10–20 μm) are of comparable size in all the samples (see Fig. 2), whereas, as the hold period is increased, the number of fine 211 particles (2–3 μm) are observed to be decreased. The volume fraction of 211 phase as determined from the photographs was also seen to decrease as the hold time is increased as shown in Fig. 3.

In this work, single crystal MgO substrates were used during melt texturing to prevent the loss of liquid phase during the experiments. It can be seen from the 211 volume fraction data (Fig. 3), that the volume fraction is larger in shorter hold period samples than in longer period of hold samples. Had the liquid phase been lost with time, one would expect the opposite, i.e. the longer the period of hold, the greater should be the loss of liquid and higher should be the 211 volume content. So the observed differences in 211 volume content are believed to be due to the 123 growth rate differences caused by the 211 particle size distribution prior to 123 nucleation and growth.

Fine 211 particles dissolve in liquid more quickly than large 211 particles during 123 formation, due to the higher surface free energy of fine particles. The 123 growth rate, which primarily depends upon the 211 particle dissolution rate,[24] can be expected to increase as the 211 particle dissolution rates are increased. 211 particles are finer in short hold time samples due to reduced coarsening, and hence, the 123 growth rates are expected to be higher. The faster the 123 growth rate is, the higher is the probability of

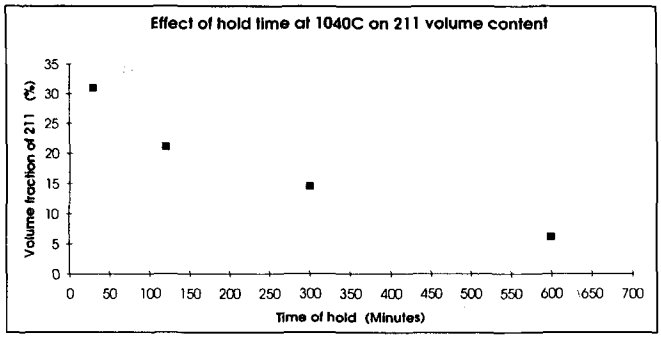

Fig. 3. 211 volume fraction in the same samples as in Fig. 2 plotted as a function of hold time.

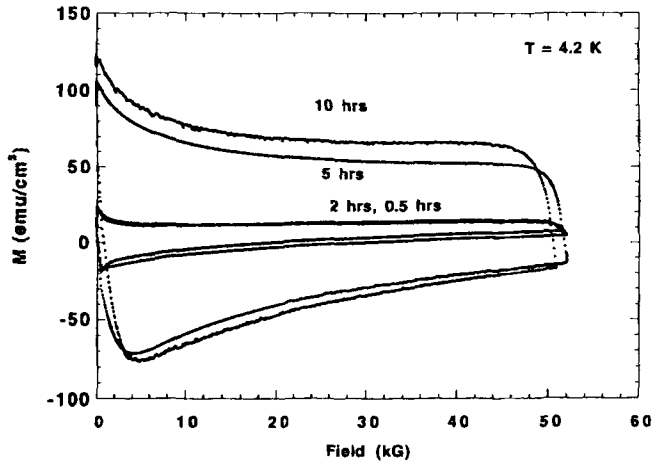

Fig. 4. Magnetization curves generated from 100 mg powders of each of the samples shown in Fig. 2 at 4.2K. A large increase in ΔM in 10 h hold sample over 0.5 h hold sample can be seen.

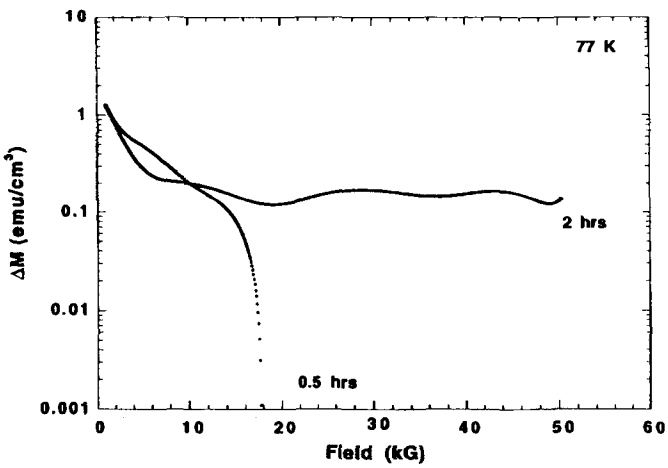

Fig. 5. A plot showing the steep fall in ΔM value of 0.5 h hold sample with magnetic field as compared to 2 h hold sample.

trapping 211 particles. Hence one sees many fine 211 particles in the final textured structure of short hold time samples because they contain many fine particles to begin with (less coarsening) and also because faster 123 growth rates trap a greater number of fine 211 particles.

As the hold time is increased, extended coarsening results, leading to fewer but larger 211 particles which is thought to reduce the 123 growth rate during

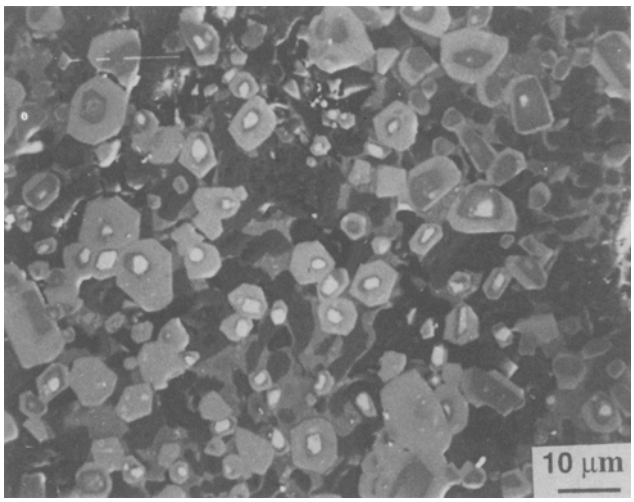

Fig. 6. Scanning electron photomicrograph showing that externally added Er 211 particles (bright cores of the particles) act as heterogeneous nucleation sites for the peritectically formed Y-211 (dark rings around the bright cores) in a Er 211 doped Y-123 pellet quenched from 1025°C after a 5 min hold period.

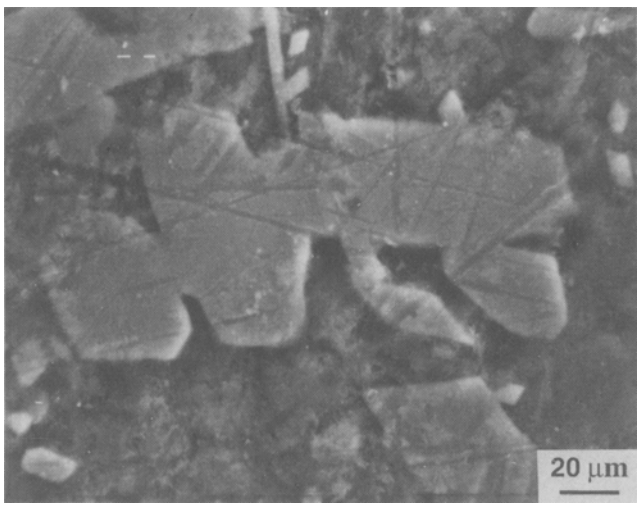

Fig. 7. Scanning electron photomicrograph showing the phenomena of 211 particle coalescence in a pure 123 pellet quenched from 1040°C after a 30 min hold period.

solidification due to lower dissolution rates and longer diffusion distances. Correspondingly, fine 211 particles are not observed in melt textured 123 held for long periods above Tp. The reduction in 123 growth rate results in less trapping of 211 by the solidifying 123, and so allows for more extensive 211 particle dissolution during solidification, and explains the absence of very large particles in the final melt textured pellet held for longer periods above Tp.

Figure 4 shows the hysteresis loops generated from powdered, oxygenated, 100 mg 123 samples of different hold times, using a vibrating sample magnetometer. All the measured powders had similar particle sizes (approx. 10–40 μm) so that the corresponding magnetization curves can be compared. From the figure, it can be seen that the intra grain J_c, which is proportional to the width of magnetization curve, increased as the hold time increased. It can be correlated with the results on zone melt textured 123 with excess 211 contents, where a decrease in J_c is observed as the 211 volume content is increased.[5] In the present case, with an increase in hold time, the 211 content is reduced, and correspondingly an increase in intra grain J_c results. This is the opposite of what one might predict simply on the basis of 211 volume percent.[15] Figure 5 shows the ΔM (loop width) vs magnetic field for 0.5 and 2 h hold samples. It can be seen that as the hold time is increased, the quality of the sample becomes better, showing a relatively stable ΔM with the field up to 5T. To understand this apparent flux pinning enhancement with an increase in hold time, transmission electron microscopy (TEM) studies are currently underway. Initial studies indicate an increase in the dislocation density as the hold time is increased and it is thought to be primarily due to an increase in undercooling which may result as a result of the hold time increase. An increase in undercooling will cause an increase in the driving force for solidification and as a result may form a higher number of dislocations.

Effect of Superheating

The affect of superheating above 1010°C on the 211 particle coarsening has been observed to be minimal.[31,33] However, Griffith et al.[31] observed a decrease in the 211 particle population density as the superheating temperature was increased. This indicates a negligible affect of an increase in driving force (ΔT) on the 211 nucleation rate.[31] It is also possible that the 211 particle dissolution rate/solubility in the liquid increases as the temperature is increased, and that the associated increased rates of coarsening mask the effects due to super heating.

EFFECT OF SECOND PHASE ADDITIONS

Additions Which Provide Heterogeneous 211 Nucleation Sites

Additions of heterogeneous nucleation sites, either in the form of excess 211, or other second phase additions, to act as nucleation sites for the peritectically produced 211, decrease the average 211 particle size. 211 particles are very effective in this manner. Jin et al. added aerosol processed 211 particles that were 0.2 μm in size, and after texturing had a 0.7 μm 211 size in the Y-123 matrix.[6] In earlier studies by McGinn et al.[5] on zone melt processed 123 with excess 211, a decrease in 211 size was observed as the added 211 amount was increased due to the added 211 providing heterogeneous nucleation sites for the peritectic 211. Figure 6 shows the microstructure of a Y-123 pellet with Er 211 additions quenched from 1025°C. The fact that most of the 211 particles in Fig. 6 contain Er-rich cores (the bright centers) indicates that the added 211 acts as a heterogeneous nucleation site for the Y-211 during Y-123 decomposition. In the absence of heterogeneous nucleation sites, the total number of nucleation events will be less as compared to when they are present. Corre-

spondingly, the particle size will be larger in the absence of heterogeneous nucleation sites. But by providing the heterogeneous nucleation sites, the number of nucleation events are increased and a smaller 211 particle size will result.

Additions Which Affect the 211 Size by a Chemical Interaction

Additions of Pt and PtO_2 have been found to lead to decreases in 211 size and also to change the morphology of 211 into particles with a very high aspect ratio by reducing the coarsening rate by decreasing the energy of the 211/liquid phase interface.[10,34] In techniques such as QMG and MPMG, Pt additions result from corrosion of the Pt crucible by the melt, whereas in other techniques discrete additions are required. $BaSnO_3$ additions to 123 were also found to refine 211 parlicles.[35] The refinement is caused by a different mechanism where $BaSnO_3$ acts as Y sink, forming Y-Ba-Sn-O precipitates in the 123 melt textured microstructure.[36] Gawalek et al.[37] have examined the effects of $BaTiO_3$ additions on melt processing of 123. Average 211 particle size was reported to be 15–20 μm, and formation of Y-Ba-Ti-O phase inclusions in 123 matrix was noted. Cerium oxide additions in melt processed 123 have produced considerable refinement in the 211 particle size, as reported by Ogawa et al.[38] They proposed that cerium oxide acts as grain growth inhibitor for 211 particles and hence a small size 211 can be obtained by modifying surface energy. Additions of $BaCeO_3$ to 123, similar to PtO_2 additions, were also found[39] to decrease the 211 particle size and change the morphology to more acicular shape.

211 PARTICLE COARSENING

211 particle size can increase due to coarsening in the liquid above the peritectic temperatures by two means: i) Ostwald ripening, and ii) particle coalescence. The evidence for Ostwald ripening to occur has been obtained by several researchers.[31,40,41] Both reaction controlled and diffusion controlled coarsening mechanisms were suggested to take place in the case of 211 particle coarsening in liquid.[31,40] It was observed by Varanasi et al.[40] that 211 particles have anisotropic growth rates and as a result a rod-like morphology of the particles is obtained when extended coarsening was allowed to take place. It has also been found that the 211 particle coarsening rate is reduced drastically in the presence of Pt additions but increases in the case of excess liquid phase or Al_2O_3 additions.[42] It appears that the 211/liquid surface energy variations as a result of the second phase additions can influence the coarsening rates to a great extent. 211 morphological changes introduced as a result of second phase additions can also influence the coarsening rates.

Several 211 particles in a close proximity can coalesce to form one single large particle and thereby reduce the total surface energy. That such a process can occur with 211 was first suggested by Izumi et al.[25] and evidence of this has been reported by Varanasi et al.[36] Figure 7 shows the microstructure of a quenched pure 123 pellet held for 30 min at 1040°C. It can be seen that more than five 211 particles are in the process of coalescing to form one single large particle. The extent of particle coalescence is hard to assess, as after it has occurred, one cannot distinguish it from a single large particle. Particle coalescence can also be affected by the presence of second phase additions similar to Ostwald ripening. Such an affect was noted by Varanasi et al.[36] when 211 particle coalescence was not observed to take place in the presence of Pt in the system.

CONCLUSIONS

A great deal of control over the 211 particle size in 123 has been achieved as a result of the various experiments conducted to understand 211 particle formation and growth during 123 melt processing. The inevitable presence of 211 phase in 123 can be used for advantage (e.g. enhancing J_c) by refining its particle size. Many processing techniques (e.g. QMG, MPMG, PMP, zone melting, and SLMG etc.) have been developed to produce 123 with 211 particles in various size ranges. 211 particle size can also be refined by manipulating the processing steps, e.g. heating rate, hold time, starting 123 grain size, etc. The selection of a second phase addition (excess 211, PtO_2, $BaSnO_3$, CeO_2, etc.) can greatly affect the 211 particle size in melt processed 123. The extent of Ostwald ripening and 211 particle coalescence have to be minimized to produce a fine 211 particle size.

ACKNOWLEDGMENTS

The authors wish to acknowledge the support of this work by the Midwest Superconductivity Consortium (U.S. Department of Energy Contract DE-FGO2-90ER45427).

REFERENCES

1. S. Jin, T.H. Tiefel, R.C. Sherwood, M.E. van Dover, R.B. Kammlott, G.W. Fastnacht and H.D. Keith, *Appl. Phys. Lett.* 52, 2074 (1988).
2. K. Salama, V. Selvamanickam, L. Gao and K. Sun, *Appl. Phys. Lett.* 54, 2352 (1989).
3. M. Murakami, M. Morita and N. Koyama, *Jpn. J. Appl. Phys.* 28, L1125 (1989).
4. P.J. McGinn, W. Chen, N. Zhu, M. Lanagan and U. Balachandran, *Appl. Phys. Lett.* 57, 1455 (1990).
5. P. McGinn, N. Zhu, W. Chen, S. Sengupta and T. Li, *Physica C* 176, 203 (1991).
6. S. Jin, G.W. Kammlott, T.H. Tiefel, T.T. Koldas, T.L. Ward and D.M. Kroeger, *Physica C* 181, 57 (1991).
7. M. Murakami, *Modern Phys. Lett. B* 4, 163 (1990).
8. D.F. Lee, V. Selvamanickam and K. Salama, *Physica C* 202, 83 (1992).
9. S. Sengupta, D. Shi, Z. Wang, A.C. Biondo, U. Balachandran and K.C. Goretta *Physica C* 199, 43 (1992).
10. N. Ogawa, I. Hirabayashi and S. Tanaka, *Physica C* 177, 101 (1991).
11. S.H. Wang, Z.X. Li, D.X. Pang, M. Suenaga, D.O. Welch, S. Jin and T.H. Tiefel, *Physica C* 168, 185 (1990).
12. P. McGinn, W. Chen, N. Zhu, L. Tan, C. Varanasi and S. Sengupta, *Appl. Phys. Lett.* 59, 120 (1991).
13. O.F. Schilling, Y. Yang, C.R.M. Grovenor and C. Beduz, *Physica C* 170, 123 (1990).
14. Z. Wang, A. Goyal and D.M. Kroeger, *Phy. Rev. B* 47, 5373

(1993).
15. M. Murakami, S. Gotoh, N. Koshizuka, S. Tanaka, T. Matsushita, S. Kambe and K. Kitozawa, *Cryogenics* 30, 390 (1990).
16. H. Fujimoto, M. Murakami and N. Koshizuka, *Physica C* 203, 103 (1992).
17. C.A. Bateman, L. Zhang, H.M. Chan and M.P. Harmer, *J. Amer. Ceram. Soc.* 75, 1281 (1992).
18. T. Izumi, Y. Nakamura and Y. Shiohara, *J. Mater. Res.* 7, 1621 (1992).
19. S. Jin., R.C. Sherwood, E.M. Gyorgy, T.H. Tiefel, R.B. van Dover, S. Nakahara, L.F. Schneemeyer, R.A. Fastnacht and M.E. Davis, *Appl. Phys. Lett.* 54, 584 (1989).
20. K. Salama, V. Selvamanickam, L. Gao and K. Sun, *Appl. Phys. Lett.* 54, 2352 (1989).
21. M. Murakami, M. Morita, K. Doi and K. Miyamoto, *Jpn. J. Appl. Phys.* 28, 1189 (1989).
22. H. Fujimoto, M. Murakami, S. Gotoh, N. Koshizuka, T. Oyama, Y. Shiohara and S. Tanaka, *Advances in Superconductivity 2* (Springer-Verlag, 1990), p. 285.
23. P.J. McGinn, W. Chen and M.A. Black, *Physica C* 161, 198 (1989).
24. M.J. Cima, M.C. Flemings, A.M. Figueredo, M. Nakade, H. Ishii, H.D. Brody, and J.S. Haggerty, *J. Appl. Phys.*72, 179 (1992).
25. T. Izumi and Y. Shiohara, *J. Mater. Res.* 7, 16 (1992).
26. Z. Lian, Z. Pingxiang, W. Keguang, W. Jirong and W. Xiaozu, *Supercond. Sci. Tech.* 3, 490 (1990).
27. C. Varanasi, S. Sengupta, P.J. McGinn and Donglu Shi, *Appl. Superconductivity* 2, 117 (1994).
28. D. Shi, S. Sengupta, J.S. Luo, C. Varanasi and P.J. McGinn, *Physica C* 213, 179 (1993).
29. C. Varanasi, P.J. McGinn, V. Pavate and E.P. Kvam, *Physica C* 221, 46 (1994).
30. C. Varanasi and P.J. McGinn, *Materials Lett.* 17, 205 (1993).
31. M.L. Griffith, J.W. Halloran and R.T. Huffman, *J.Mater. Res.* in press.
32. J. Rignalda, X. Yao, D.G. McCartney, C.J. Kiely and G.J. Tatlock, *Materials Lett.* 13, 357 (1992).
33. C. Varanasi and P.J. McGinn, unpublished.
34. C. Varanasi and P.J. McGinn, *Physica C* 207, 79 (1993).
35. P. McGinn, W. Chen, N. Zhu, C. Varanasi, L. Tan and D. Balkin, *Physica C* 183, 51 (1991).
36. C. Varanasi, M.A. Black and P.J. McGinn, *Supercond. Sci. Technol.* 7, 10 (1994).
37. W. Gawalek, T. Habisreither, K. Fischer, G. Bruchlos and P. Gornert, *Cryogenics* 33, 65 (1993).
38. N. Ogawa and H. Yoshida, *Advances in Superconductivity IV* (1991), p. 455.
39. C.J. Kim, private communication.
40. C. Varanasi and P.J. McGinn, *J. Electron. Mater.* 22, 1251 (1993).
41. T. Izumi, Y. Shiohara and Y. Nakamura, *Proc. Intl. Workshop on Superconductivity* (Pittsburgh, PA: Materials Research Society, 1992), p. 280.
42. T. Izumi, Y. Nakamura and Y. Shiohara, preprint.